An Overview of the April 28, 2014 Tornado Outbreak

Chris Lisauckis

November 2018

1. Introduction

The tornado outbreak of 28 April 2014 affected the lower Mississippi and Tennessee Valleys, producing a total of fifty-two tornadoes, including five EF0, twenty-six EF1, twelve EF2, eight EF3, and one EF4 on the Enhanced Fujita Scale. It was the largest tornado outbreak in 2014 and remains one of the largest outbreaks in the United States since the infamous 27 April 2011 Super Outbreak. Unfortunately, 15 fatalities were reported along with 203 injuries. The state of Mississippi was hardest hit, including 11 unfortunate fatalities that occurred during the mid-afternoon and early evening hours. The event consisted primarily of corridors of classic and high precipitation supercell thunderstorms which moved to the northeast within the right exit region of the 300 mb upper tropospheric jet streak. Uniquely, the outbreak region was also positioned within the right entrance region of a 500 millibar jet streak associated with a potent shortwave trough. Due to strong return flow of low level moisture from the Gulf of Mexico, the event featured a potent atmospheric thermodynamic field. When this highly buoyant airmass became juxtaposed with the appreciable kinematic envelope associated with the return branch of the transverse thermally indirect ageostrophic circulation of an especially powerful 300 mb jet, a highly conducive pattern developed for tornadic supercell storms.

The surface low pressure center which developed in association with this event, tracked through Kansas and into northern Missouri and Iowa. This low pressure track has been associated with many significant tornado outbreaks in the eastern United States, including: April 3, 1974 - November 24, 2001 - March 1, 2007 - and April 15, 2011. The surface pressure field,

associated with the upper air height falls, remained sufficient for severe storm development well into the deep south. Moreover, as is common with major tornado outbreaks in the southeastern United States, the cessation of diabatic solar insolation did little if anything to quell the event due to the strength of thermodynamic and kinematic parameters involved (i.e. April 27, 2011 - February 5-6, 2008 - November 21-22, 1992 etc.). This case analysis features primarily observational data provided by radiosonde, NOAA ASOS, and WSR-88D Nexrad. Storm Prediction Center mesoanalysis archive data was also used to help bridge data gaps when necessary. A rare High Risk for severe thunderstorms was issued by the Storm Prediction Center at a Special 1919 UTC April 28 Day 1 Outlook for parts of Mississippi and northwest Alabama (Fig. 1.1). This risk was upgraded from moderate based specifically upon the increasing risk of strong and violent tornadoes across the region.

2. Synoptic Features

A large negatively tilted longwave trough, associated with the upper tropospheric polar jet, was located over the central and eastern United States the afternoon of April 28. The base of the 300 millibar trough was positioned due west of northern Mississippi and northern, AL (Fig. 2.1). Moreover, 300 mb was also the mandatory level which featured the greatest meridional height gradient at the base of the trough, marking an important region of vorticity generation. This vorticity was then advected rapidly downstream and over portions of the severe weather threat area, including Mississippi and Alabama. A glancing jet pattern was observed in this case at both 300 and 500 mb, meaning that the upper level jet glanced the core of the outbreak region on the north and west side, while the jet core remained primarily removed from the outbreak region. This glancing upper jet configuration is the most common of the five types of jet models which have been identified as nosing, glancing, overrunning, intersecting, and diffuse (preliminary

dissertation research by author). This negatively tilted longwave trough featured an elongated 500 mb shortwave which stretched from the Red River valley east into western Mississippi (Fig. 2.2). Negatively tilted troughs have the potential to generate greater absolute vorticity due to rapid poleward transport of relative vorticity on their eastern side. Also, the geometry produced by this negative tilt allows a greater amount of upper level cold air to advect overtop the existing warm sector airmass.

3. Atmospheric Thermodynamics

12 UTC atmospheric soundings from both Birmingham, AL (KBMX) (Fig. 3.1) and Jackson, MS (KJAN) (Fig. 3.2) the morning of April 28th indicated mean layer CAPE (MLCAPE) values of 1502 and 1556 Jkg^{-1} respectively. These observations served as a strong indication of the available conditional instability which would continue to increase during the afternoon hours. As a result, 18 UTC soundings from both KBMX (Fig. 3.3) and KJAN (Fig. 3.4) indicated a further increase in instability, with MLCAPE values increasing to 1965 Jkg^{-1} and 2522 Jkg^{-1} respectively. The level of maximum buoyancy lifted index (LMB LI) for the 18 UTC soundings were -8C observed at 350 mb at KBMX, and -10C observed at 350 mb at KJAN. Interestingly, the fact that the level of maximum buoyancy was observed at the same height for both sounding locations likely reflects a common source of mid/upper level lapse rates which were being advected overtop the threat region. A broad warm sector, extending east from the Mississippi River well into Georgia, provided a broad slab of instability for long track supercells to operate within, and prevented cells from outrunning the warm sector airmass. The author has observed that most significant tornado outbreaks in Mississippi, Alabama, and Tennessee occur with a warm sector which is approximately 482 km (300 miles) in width (Fig. 3.5). Also of interest is a region of anomalously high daily maximum temperatures across southern Texas during the

previous afternoon. This included San Antonio reaching a high temperature of 99 degrees, and 100 degrees at Brownsville. This southern Texas warm anomaly has been observed the day before numerous significant tornado events and is certainly noteworthy (Matt Grantham - NWSFO Birmingham – Personal Communication).

Low level moisture advection was primarily responsible for the increase in buoyancy during the morning and early afternoon hours, resulting in markedly warmer parcel temperatures aloft at 18 UTC as compared to the 12 UTC soundings. Mid and upper level temperatures rarely cool significantly during tornado outbreaks as found by Thompson et al. (2008), and warm slightly as often as they cool. This indicates that increased buoyancy for severe storm events typically originates from low level theta-e advection. CAPE values observed within the 0-3000 m layer via the 18 UTC soundings were 74 J/kg at KBMX and 86 J/kg at KJAN, signifying sufficient level instability values for significant tornadoes (Davies 2002). However, reduced 0-3000 m CAPE values are often observed in southeastern U.S tornado events when compared to events on the Great Plains. This is primarily attributed to weak low level lapse rates associated with an abundance of gulf moisture (Jackson and Brown 2009). Moreover, relative humidity values within the LCL-LFC layer were between 80-90% throughout the event, lending less opportunity for dry air entrainment to adversely affect buoyancy. A low LCL does not imply a low LFC, however, potent theta-e advection and diabatic heating produced sufficient low level lapse rates to permit an LFC and LCL which were separated by no more than 200 meters within the primary corridor of tornadic supercell development. Height of the mean layer lifted condensation level (MLLCL) at 18 UTC, portrayed on the KJAN radiosonde was 1102 m, a seemingly unfavorable value for a major tornado outbreak in the deep south. This LCL height remained constant throughout the day, when not contaminated briefly by outflow and precipitation, as confirmed

via KJAN and KTUP ASOS LIDAR ceilometer observed cloud base heights of 1188 and 1096 m respectively during the afternoon hours. Theses observations lent credence to the idea that LCLs were rather homogenous across the High Risk outlook area during the tornado outbreak.

A strong gradient in 700 mb specific humidity was observed in western Mississippi, approximately 185 km (115 miles) west of the ongoing tornado outbreak at 21 UTC as seen in Fig. 3.6. This feature is believed to indicate the location where the elevated mixed layer (EML) entered the severe weather threat region, providing a means of releasing additional convective instability and aiding in explosive supercell development. The author has observed this signature numerous times during severe weather events across the U.S. and has used it to add a layer of confidence regarding the spatiotemporal forecast of the most intense convection. Among the mandatory levels, this pattern consisting of a couplet of high and low relative humidity, is often observed approximately 160 km (100 miles) east of either the 500 or 700 mb relative humidity couplet. The elevated mixed layer is known to be an excellent source of very dry upper level air originating over the Rocky Mountains of the United States or the arid highland plateau region of northern and central Mexico. Aside from providing a means of convective/potential instability release, the EML often promotes a slight capping inversion which acts to curtail the development of unnecessary shallow convection that can adversely modify both the thermodynamic and kinematic environments. This capping inversion is typically not strong enough to prevent severe thunderstorm development over the eastern/southeastern states as it is over the U.S. Great Plains region, where many major tornado outbreaks have been preempted in this manner.

4. Kinematic Parameters

A detailed wind field analysis was undertaken in attempt to better understand the way in

which supercell storms were able to produce intense (EF3+) tornadoes. Moreover, it is possible that subtle recurring details within the atmospheric wind field can provide the necessary discriminators to accurately assess a given tornado threat. Buoyancy acts as clay and wind shear the potter, from which there are many possible resultant shapes and sizes. The 28 April outbreak was different than most which occur in the southeastern United States during peak tornado season in that there was a very pronounced weakness in the mid and upper level storm relative wind field. Specifically, it was noted that the surface storm relative wind was stronger than the 6 and 9000 m storm relative wind. Generally, this pattern tends to produce short track tornadoes, with tornado strength hinging upon other elements within the atmospheric parameter space. Although upper level storm relative winds were not overly favorable, the storm motion dot was still sufficiently removed from the hodograph trace to remain well within the favorable spectrum. Thankfully, this weakness likely aided in preventing tornadoes from being especially long track. The longest track tornado of the event was an EF4 which tracked 53 km (33 miles) through Leake, Attala, and Winston Counties in Mississippi including the city of Louisville, sadly resulting in 10 fatalities. Perhaps it is easy to hypothesize why an event does not "pan out" the way we often anticipate in hindsight. Therefore, the discourse provided here is up for debate. Dozens of mid-latitude troughs pass across the U.S. yearly, many times without an event similar to 28 April occurring within the span of many years. It takes a highly unique tornadic environment to produce extraordinarily long track violent tornadoes such as those observed on April 27, 2011 or April 3, 1974.

Fig. 4.1. is a hodograph constructed from the Columbus, MS (KGWX) WSR-88D VWP observed winds Fig. 4.2. A large area of storm relative helicity is swept out in the 0-500 m layer with a calculated value of 218 m^2/s^2, 242 m^2/s^2 within the 0-1000 m layer, and 320 m^2/s^2 from 0-

3000 m which is approximately 140% of the values observed from the 18 UTC KJAN radiosonde data. Therefore, these values are highly indicative of the potential for mesocyclonic rotation (Davies-Jones 1990). Of additional importance, is the fact that the storm relative wind vectors veer strongly with height, promoting an environment containing both strong wind shear and streamwise vorticity, the two of which cannot always be assumed to coexist. Furthermore, large hodographs cannot be assumed to coexist with strongly veering storm relative wind vectors with height, although the two often exist together. This hodograph trace shows a classic kink at 1000 m where the environmental wind profile shifts from one of primarily speed shear to one dominated by directional shear. The critical angle (Esterheld & Guilliano 2008), which is defined as the angle formed by the 10-500 m bulk shear and 10 m storm relative wind vectors, is 70 degrees in this case. In the southeast U.S., critical angles in the 50-70 degree range are common during significant tornado events (Guyer & Hart 2010). It should be noted that as with many severe storm metrics, a somewhat unfavorable critical angle may be overcome when strong instability exists. However, major tornado outbreaks are nearly always accompanied by a highly favorable critical angle.

Directional turning of the winds was not particularly strong within any layer of the troposphere. Rather, the vertical wind profile displayed a gradual veering from the surface to the tropopause, which is common among days where supercells are the dominant storm mode (i.e. February 5, 2008 and April 27, 2011) as found by Dial et al. (2010). This promotes a wind field where the numerical value of storm relative helicity strongly reflects the vertical wind profile, and adverse features such as veer-back-veer vertical wind profiles and overly dominant speed shear are non-existent. Additionally, there was a classic indention signature in the hodograph trace at 2000 m, which is believed to be the result of the cessation of strong warm air advection

within the ageostrophic lower level wind layer, along with a transformation to a veering thermal wind vector with height. The author has observed this signature often in significant tornadic environments. Warm air advection can be used as a proxy for storm relative helicity due to the cyclonic ageostrophic nature of the low level wind flow within such advective regimes.

Also indicated by the VWP generated hodograph are high tropospheric storm relative wind vectors which cross overtop the supercell initiating prefrontal trough at an angle close to 90 degrees (Fig. 4.3). This pattern promotes the advection of cascading downdraft supercell precipitation away from nearby thunderstorm updrafts, enhancing the likelihood of supercells and associated thunderstorm longevity (Dial et al. 2010). Also indicating the effectiveness of the kinematic environment to allow for long track supercells, the 9000-11000 m storm relative wind vectors did not undergo significant post-frontal backing west of the cold front as shown in Fig. 4.3 and 4.4. This structure is commonly observed in association with katafronts, wherein the primary cold frontal boundary is largely inactive and most of the warm sector precipitation is found well in advance of this boundary. This signal strongly promotes a cellular storm mode, along with strong differential advection of moist air in the lower levels and dry air in the mid and upper levels of the warm sector. Additionally, Fig. 4.4 indicates an abrupt north/south discontinuity in the upper tropospheric storm relative wind field, which has been observed by the author to indicate a corridor of increased tornado potential. It is not completely understood why the model data detects these discontinuities.

Fig. 4.5 shows a very pronounced maximum in warm air advection across central and northern Mississippi at 20 UTC, evident by the advective solenoids found in this region. Originating over the northern Gulf of Mexico, this strong warm advection was largely the result of the pronounced south-southwesterly low level jet which contained wind velocity of

approximately 50 knots. Moreover, as is associated with many tornado outbreaks, a strong isallobaric flow pattern was observed in central Mississippi and is represented by the significant cross-isobar flow in Fig. 4.6. Such an isallobaric wind can be used as a proxy for locating regions of enhanced storm relative helicity as found by Togstad (1994), because it represents the ageostrophic component of the pressure gradient force. It should be noted that an ageostropic component of the pressure gradient force can exist without their existing a katalobaric (pressure fall) tendency at a given point with respect to time. This is important because it indicates that surface pressure falls may not always accompany ongoing tornado outbreaks. Composite severe storm indices for the 28 April event included maximum significant tornado parameter (STP) values in the 2-4 range, 0-1000 m energy helicity index (EHI) of 3-5, and a severe weather threat index (SWEAT) of 500-550, all of which indicated a very favorable environment for significant and perhaps violent tornadoes. Also, the vortex value, an experimental tornado forecasting index presently under development by the author, indicated a value of 2450 in east-central MS which is indicative of EF4 tornadoes.

References

Davies, J. M., 2002: On low-level thermodynamic parameters associated with tornadic and nontornadic supercells. Preprints, *21st Conf. on Severe Local Storms,* San Antonio, TX, Amer. Meteor. Soc., 603– 606.

Davies-Jones, R. P., D. W. Burgess, and M. Foster, 1990: Test of helicity as a tornado forecast parameter. Preprints, 16th Conf. on Severe Local Storms, Kananaskis Park, AB, Canada, Amer. Meteor. Soc., 588-592.

Dial, G. L., J. P. Racy, and R. L. Thompson, 2010: Short-term convective mode evolution along synoptic boundaries. Wea. Forecasting, 25, 1430–1446.

Esterheld, J. M., and D. J. Giuliano, 2008: Discriminating between tornadic and non-tornadic supercells: A new hodograph technique. Electronic J. Severe Storms Meteor., 3 (2), 1–50.

Guyer, J. L., and J. A. Hart, 2012: Examination of WSR-88D VWP data in proximity to strong tornadoes. Preprints, *26th Conf. on Severe Local Storms,* Nashville, TN, Amer. Meteor. Soc., 62.

Jackson, J., and M.E. Brown, 2009 Sounding-Derived Low-Level Thermodynamic Characteristics Associated with Tornadic and Nontornadic Supercell Environments in The Southeast United States. *National Weather Digest,* **33**, 15-26.

Thompson, R. L., J. S. Grams, and J. A. Prentice, 2008: Synoptic environments and convective modes associated with significant tornadoes in the contiguous United States. Preprints, 24th Conf. on Severe Local Storms, Savannah, GA, Amer. Meteor. Soc., 16A.3.

Togstad, B., 1994: The Isallobaric Wind as a Forcing Function on Fields of Helicity, NWS CRH ARP 13-10/94.

Appendix

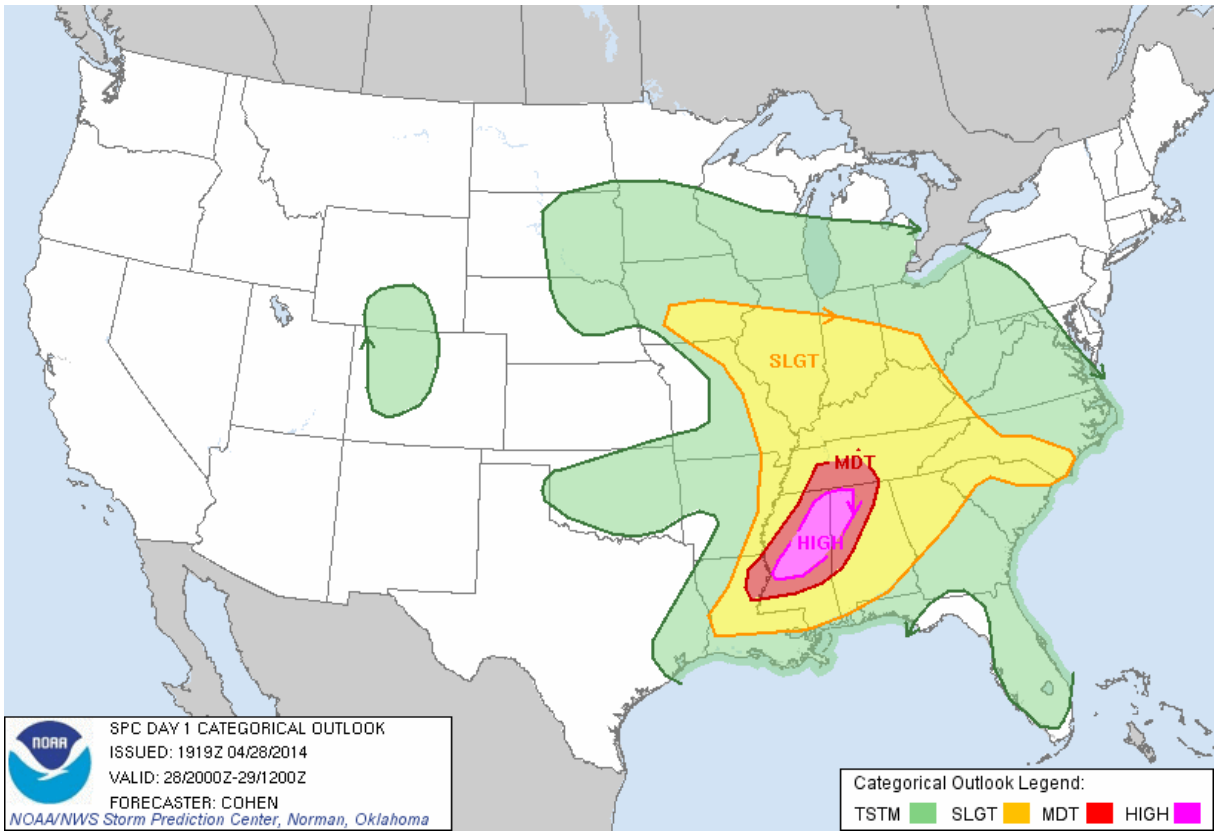

Figure 1.1. 1919 UTC 28 April 2014 UTC Day 1 severe weather outlook which upgraded parts of Mississippi and Alabama to a rare High Risk of severe, including strong and violent tornadoes. Image courtesy of SPC.

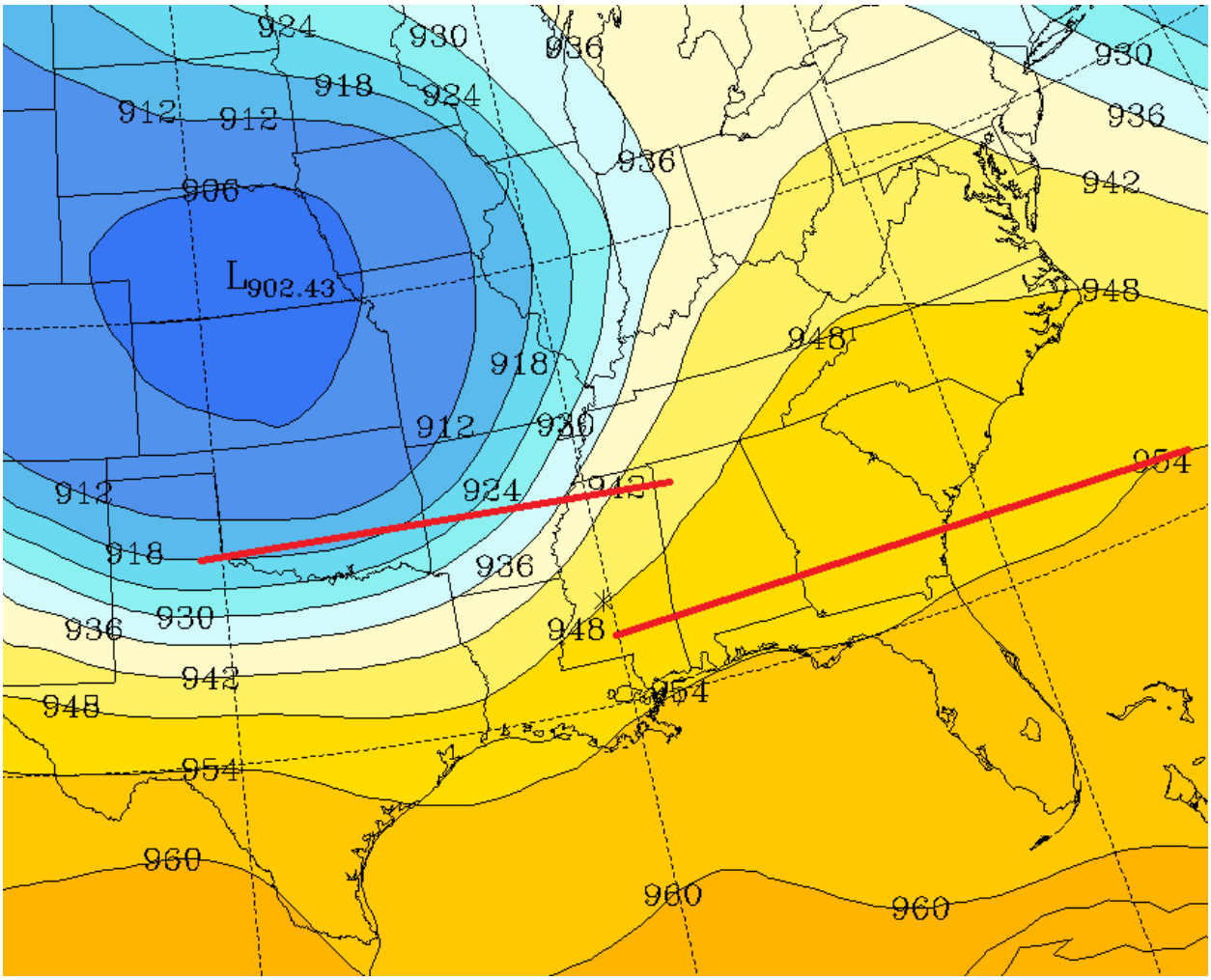

Figure 2.1. 2100 UTC 28 April 2014 300 mb plot showing trough base and downstream ridge and their position relative to northern Mississippi and Alabama. Image courtesy of the Air Resources Laboratory.

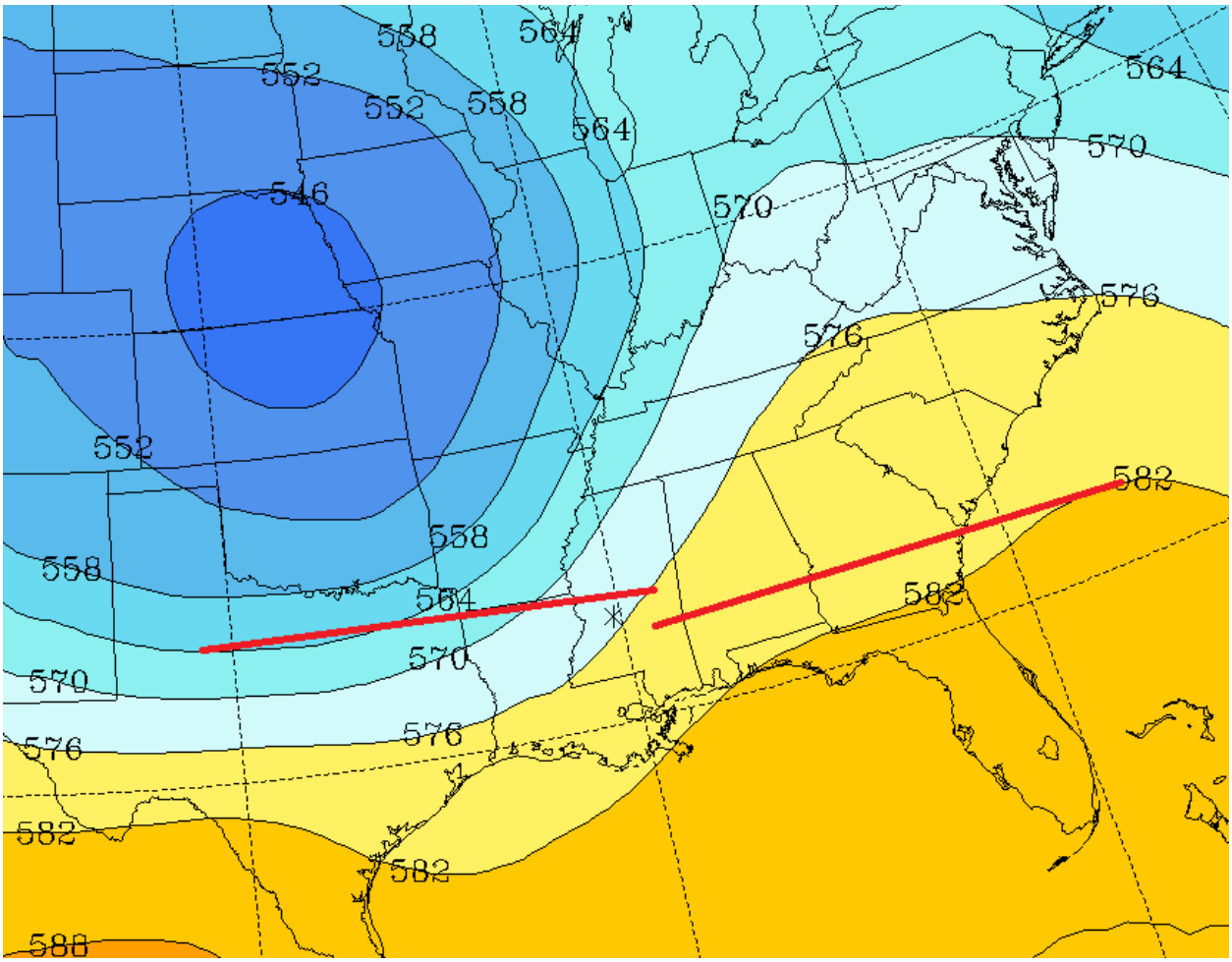

Figure 2.2. 2100 UTC 28 April 2014 500 mb plot showing trough base and downstream ridge and their position relative to central Mississippi. Image courtesy of the Air Resources Laboratory.

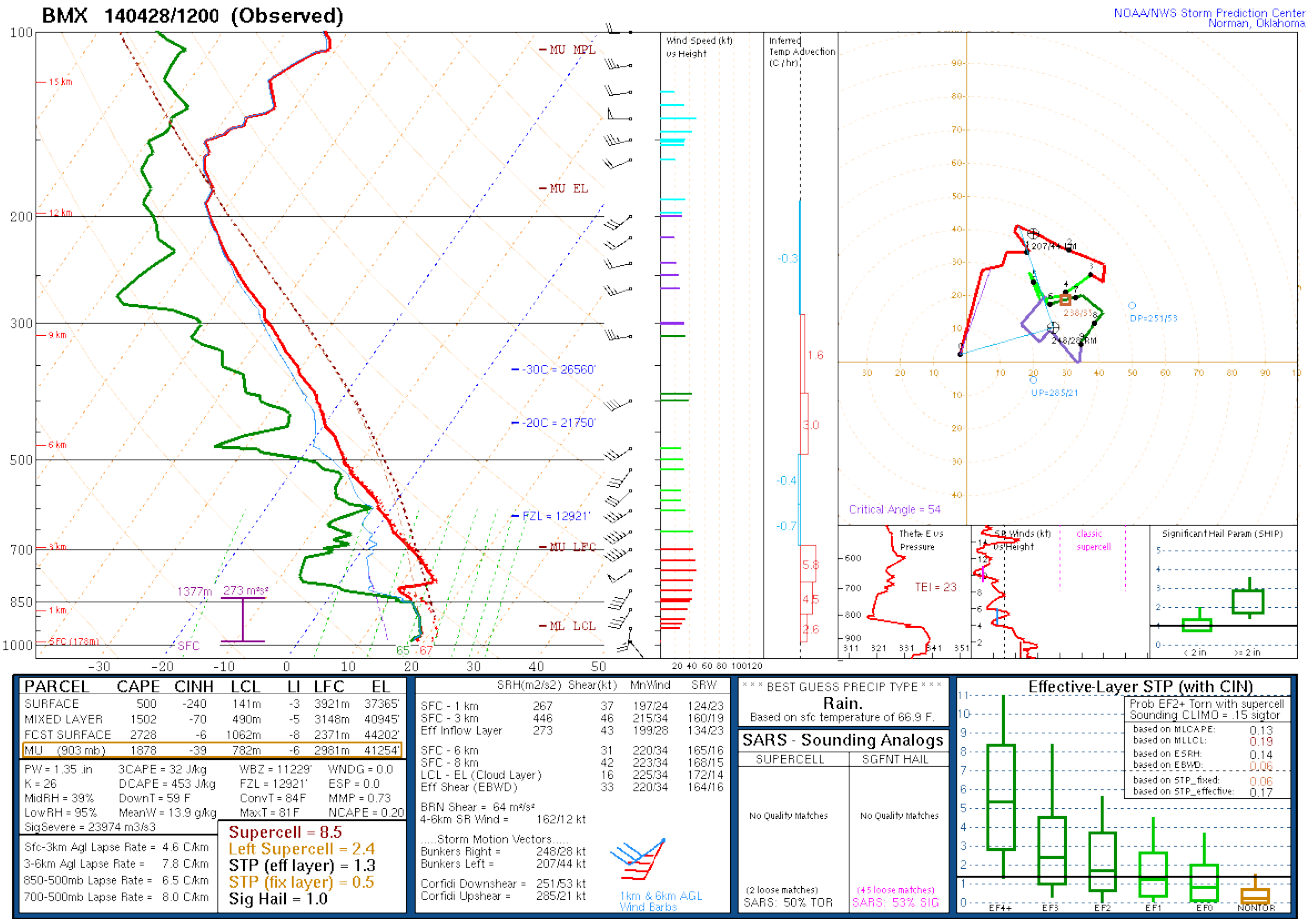

Figure 3.1. 1200 UTC 28 April 2014 radiosonde from KBMX showing instability already present. Image courtesy of the SPC.

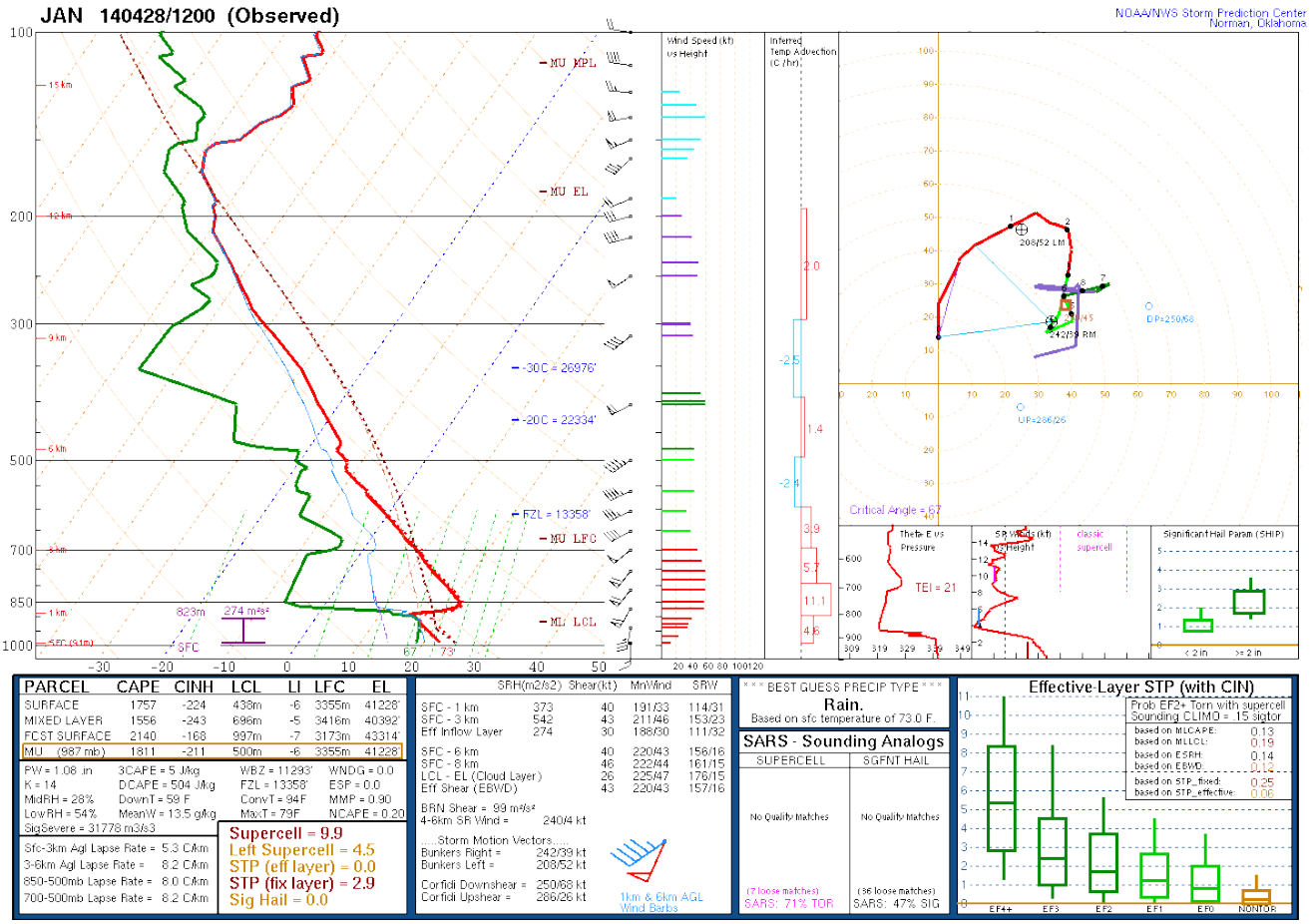

Figure 3.2. 1200 UTC 28 April 28 2014 radiosonde from KJAN showing instability already present. Image courtesy of the SPC.

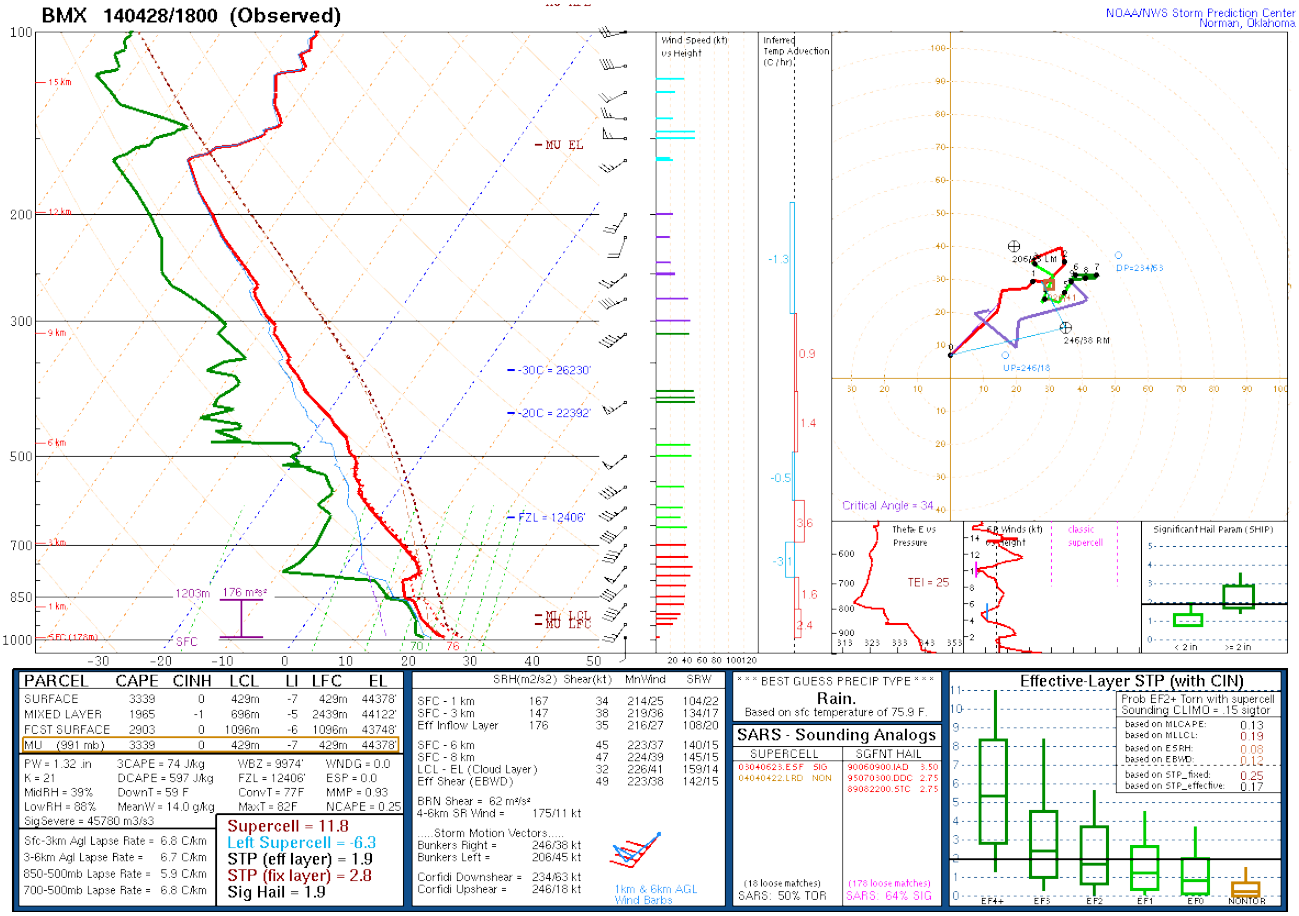

Figure 3.3. 1800 UTC 28 April 2014 radiosonde from KBMX showing increasing instability. Image courtesy of the SPC.

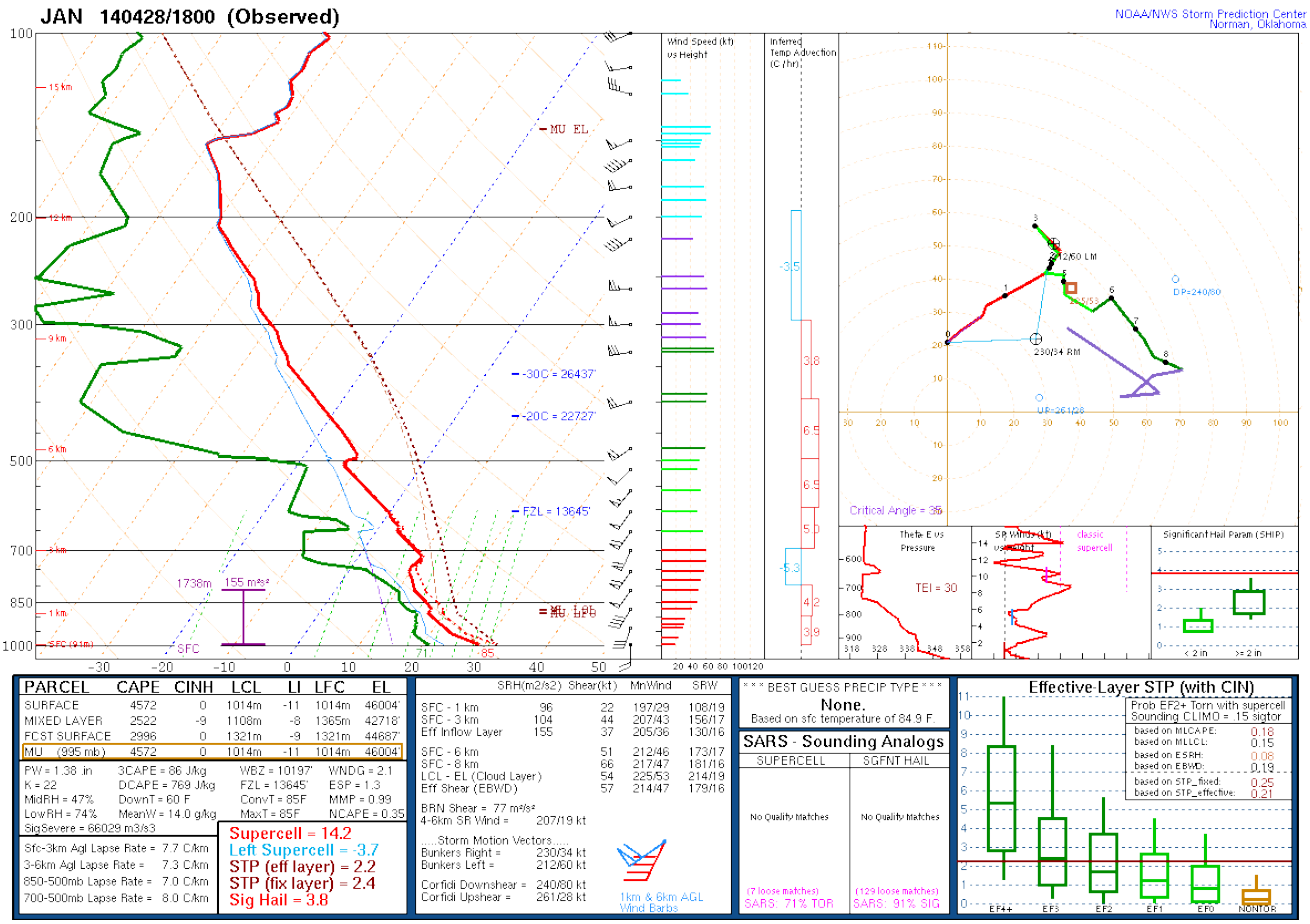

Figure 3.4. 1800 UTC 28 April 2014 radiosonde from KJAN showing increasing instability. Image courtesy of the SPC.

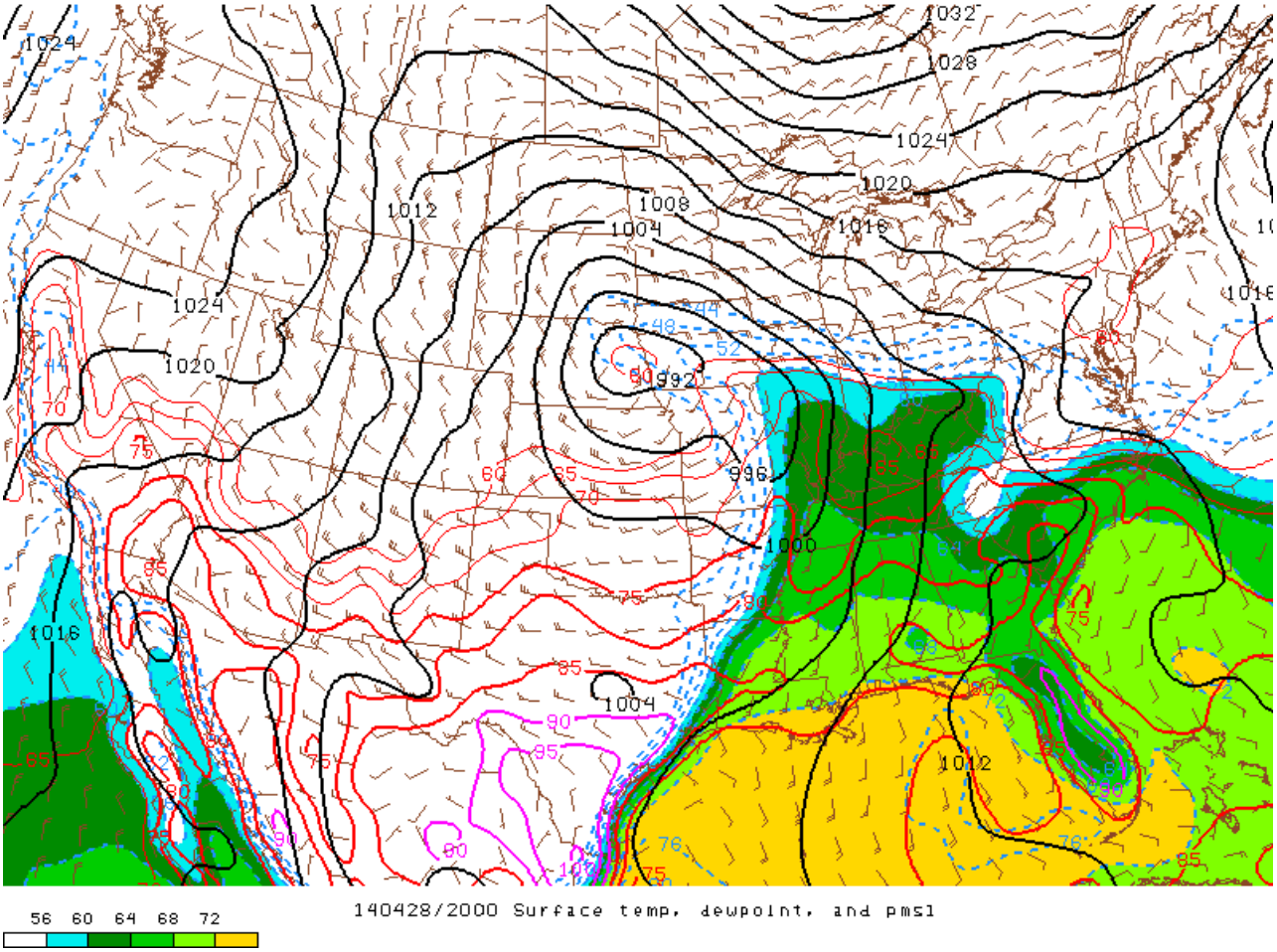

Figure 3.5. 2000 UTC 28 April 2014 surface plot showing mean sea level pressure, temperature, and dewpoint indicating the width of the warm sector airmass. Image courtesy of the SPC.

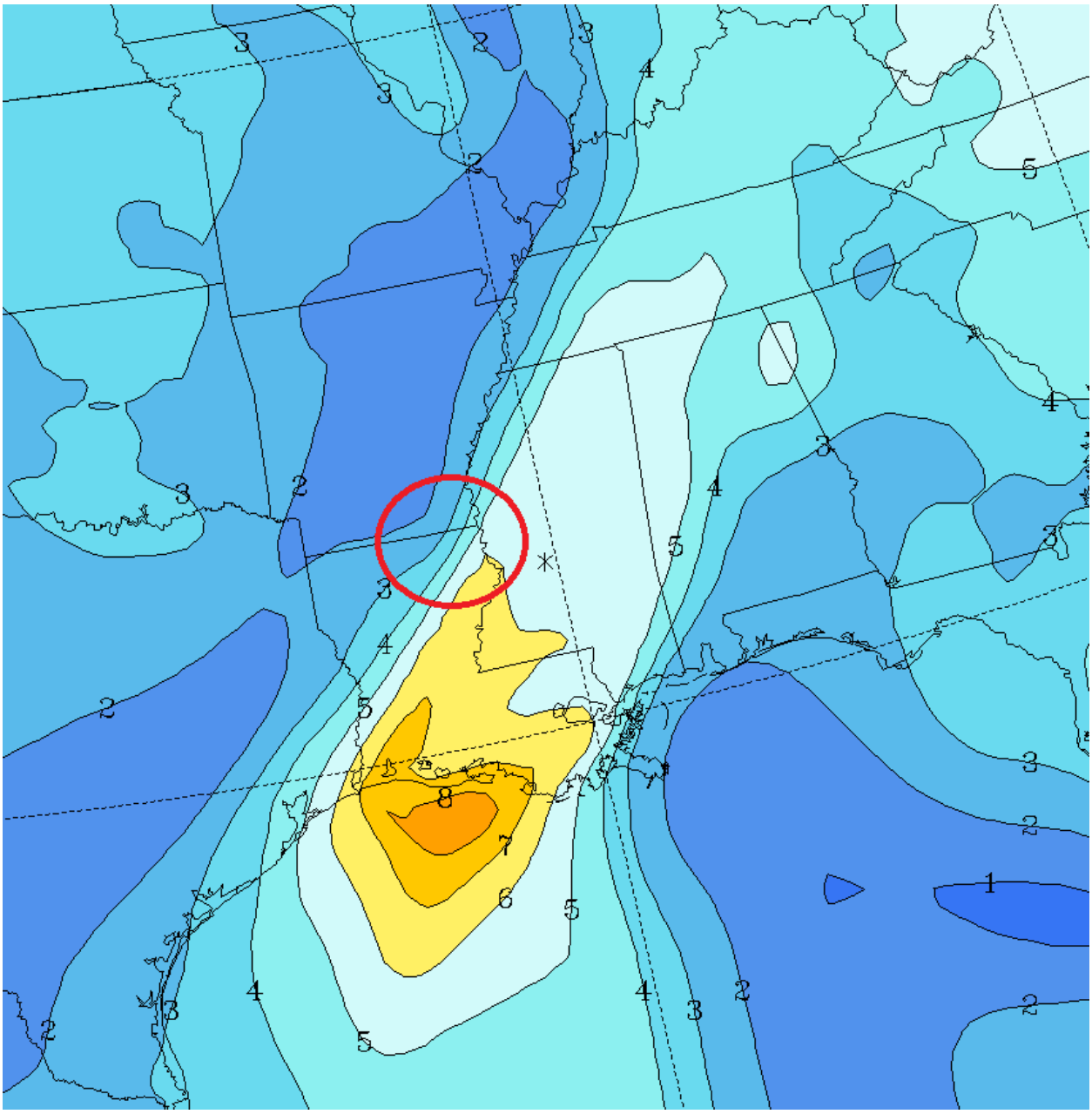

Figure 3.6. 2100 UTC 28 April 2014 700 mb plot showing a pronounced specific humidity gradient over far western Mississippi, southeast Arkansas, and northeast Louisiana. Image courtesy of the Air Resources Laboratory.

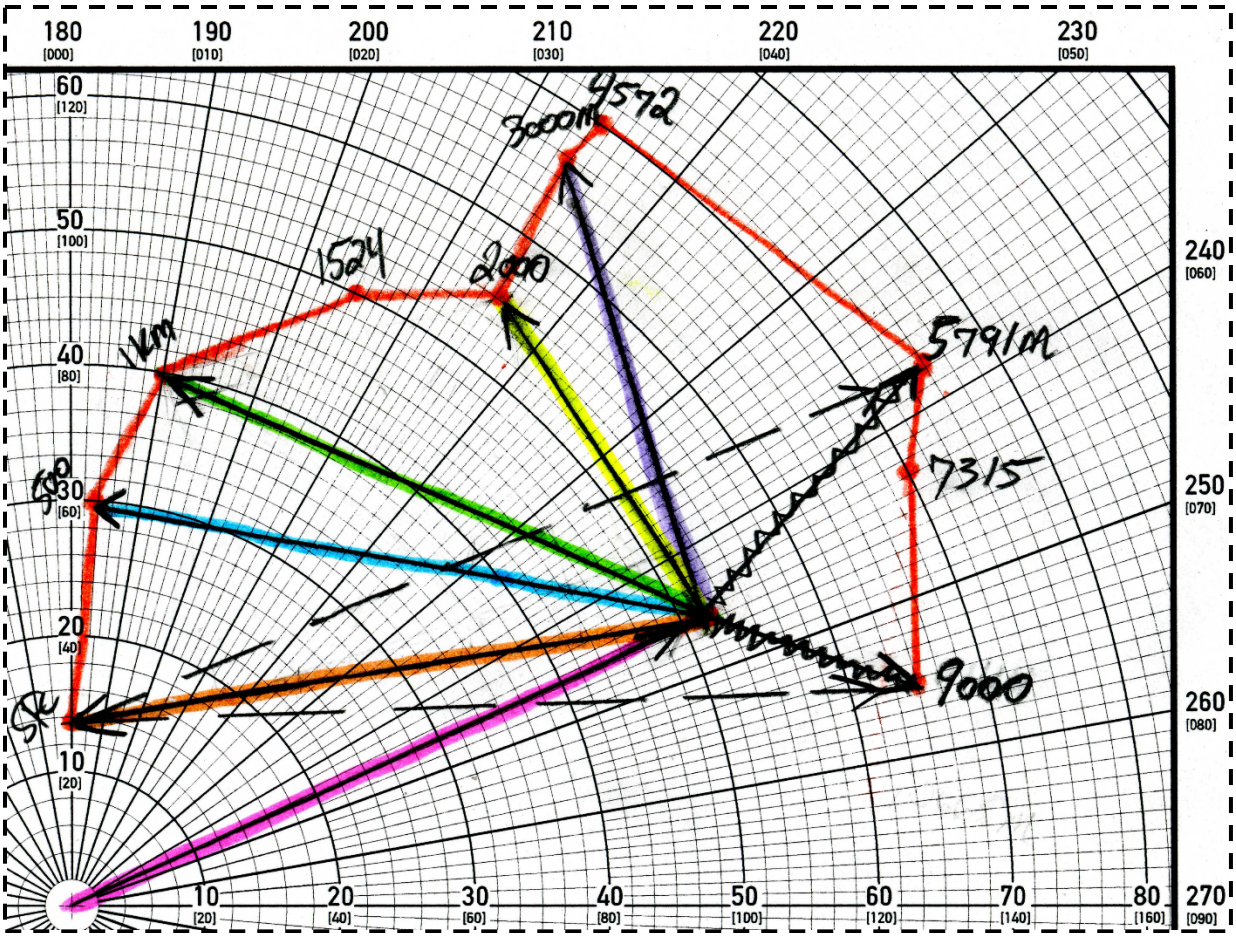

Figure 4.1. 2009 UTC 28 April 2014 Columbus, MS WSR-88D VWP generated hodograph. The solid red line is the hodograph trace, marked with increasing altitude in black, followed by: storm relative inflow vector (orange), mean wind storm motion (pink), 10-500/10-1000/10-2000/and 10-3000 meter storm relative wind vectors in blue, green, yellow, and purple respectively. Also, 10-5700 and 10-9000 meter bulk shear vectors (black dashed lines) and storm relative wind vectors (black squiggle).

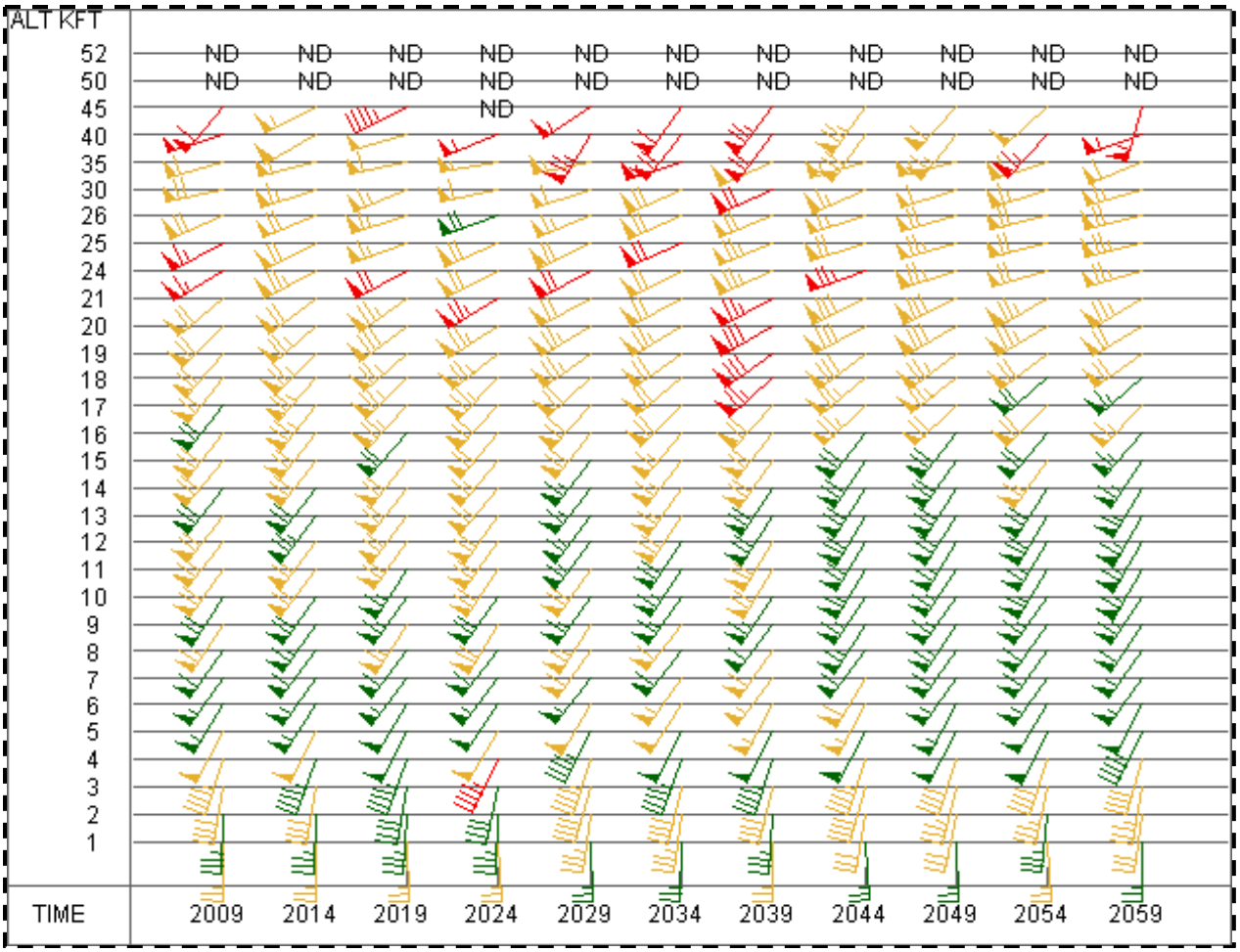

Figure 4.2. Image of the WSR 88D Vertical Azimuth Display Wind Profile originating from the Columbus, MS Nexrad on April 28, 2014. Barb colors indicate the level of confidence associated with each observation (green highest, and red the lowest). Notice how this wind profile veers gradually with increasing height, which is highly indicative of a wind profile capable of supporting supercells. Data courtesy of the NCDC.

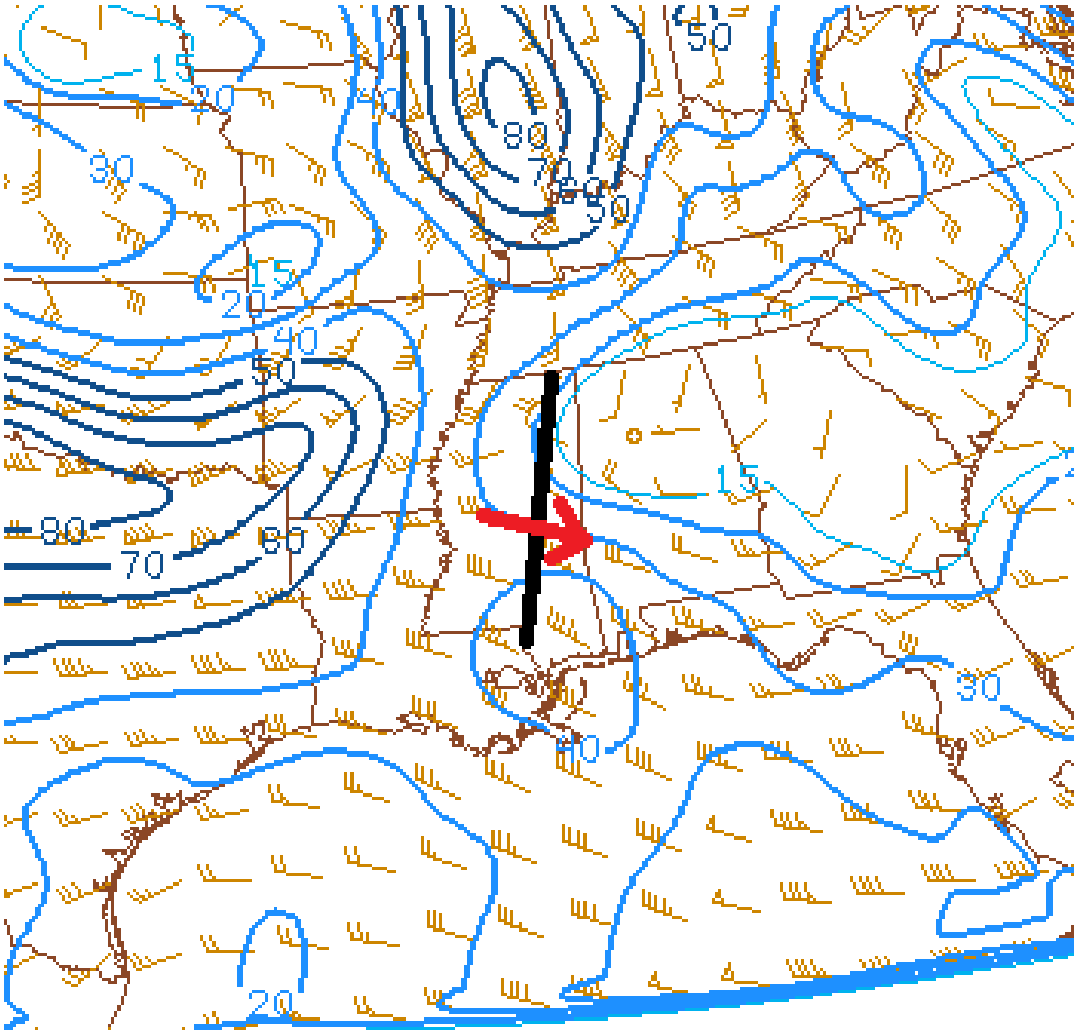

Figure 4.3. 2000 UTC 28 April 2014 figure indicating the high tropospheric storm relative wind vectors (red arrow) crossing the storm initiating prefrontal trough boundary (black line) at close to a 90 degree angle. Image courtesy of the SPC.

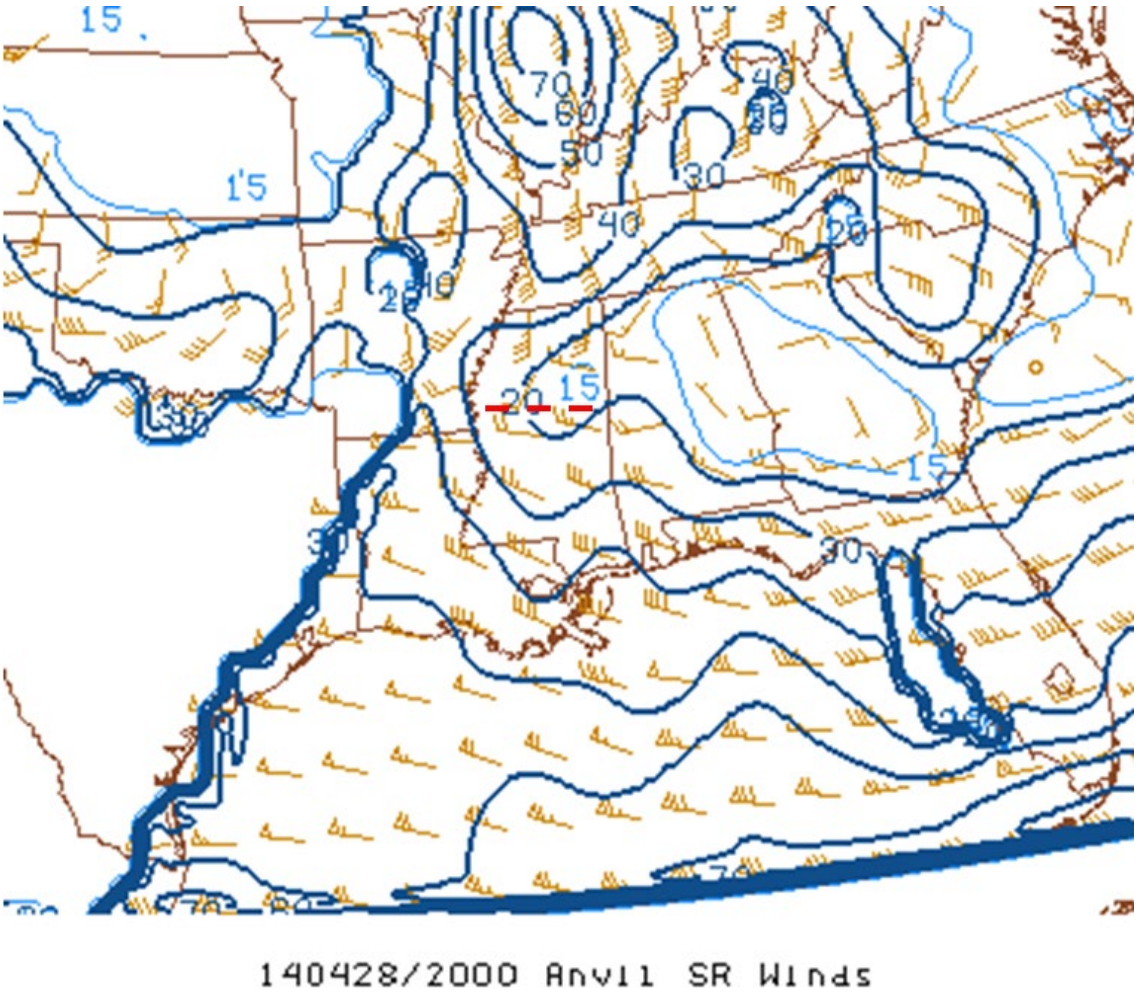

Figure 4.4. 2000 UTC 28 April 2014 figure indicating an abrupt north/south discontinuity in anvil level storm relative wind vectors (red dashes) and a corresponding corridor of supercell development. Image courtesy of the SPC.

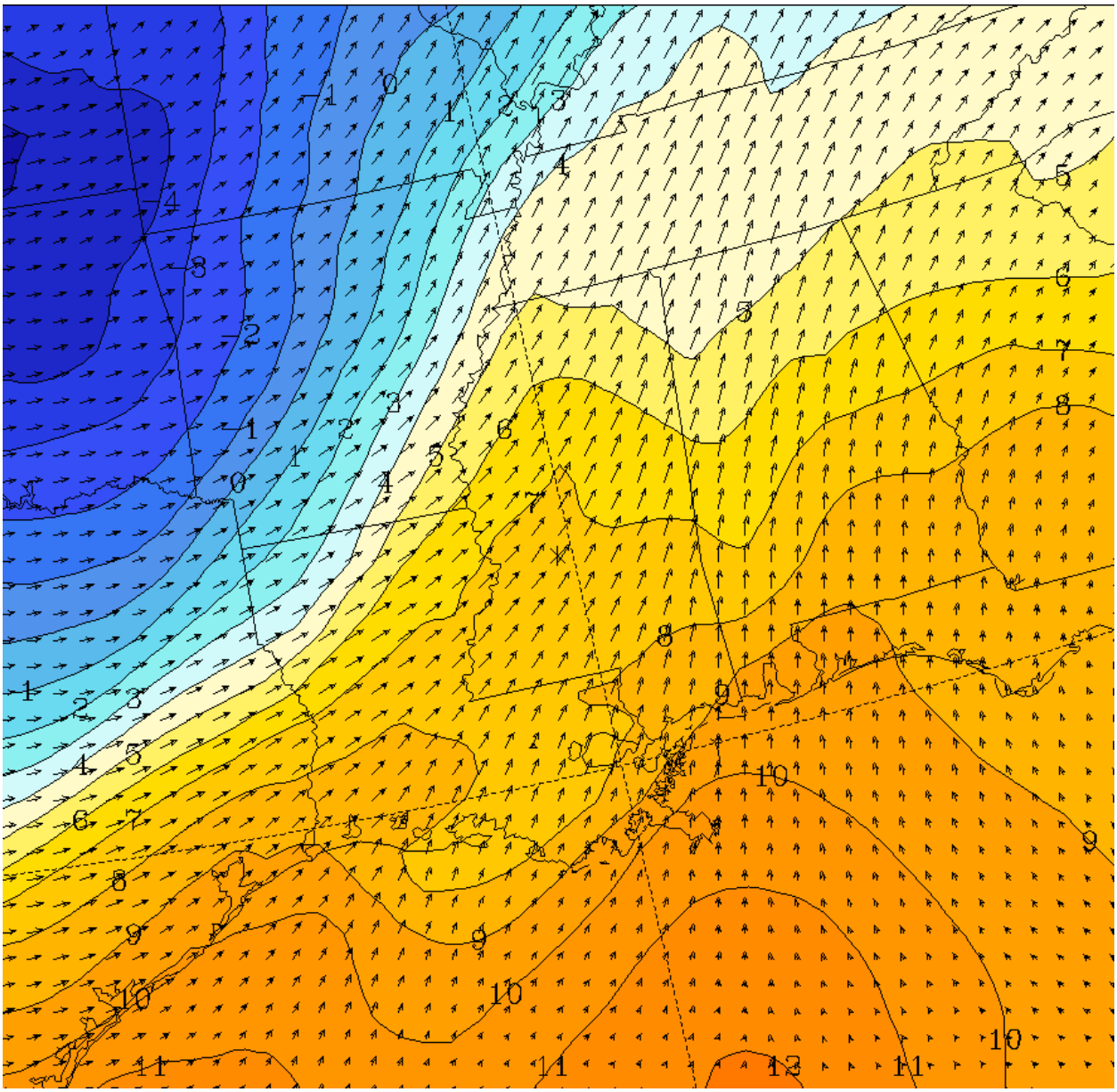

Figure 4.5. 2100 UTC 28 April 2014 plot showing 700 mb temperature field (filled color contours) and wind vectors (black arrows). Strong thermal advection is evident over portions of Mississippi and Alabama, including highly pronounced advective cusps over central and northern Mississippi. Image courtesy of the Air Resources Laboratory.

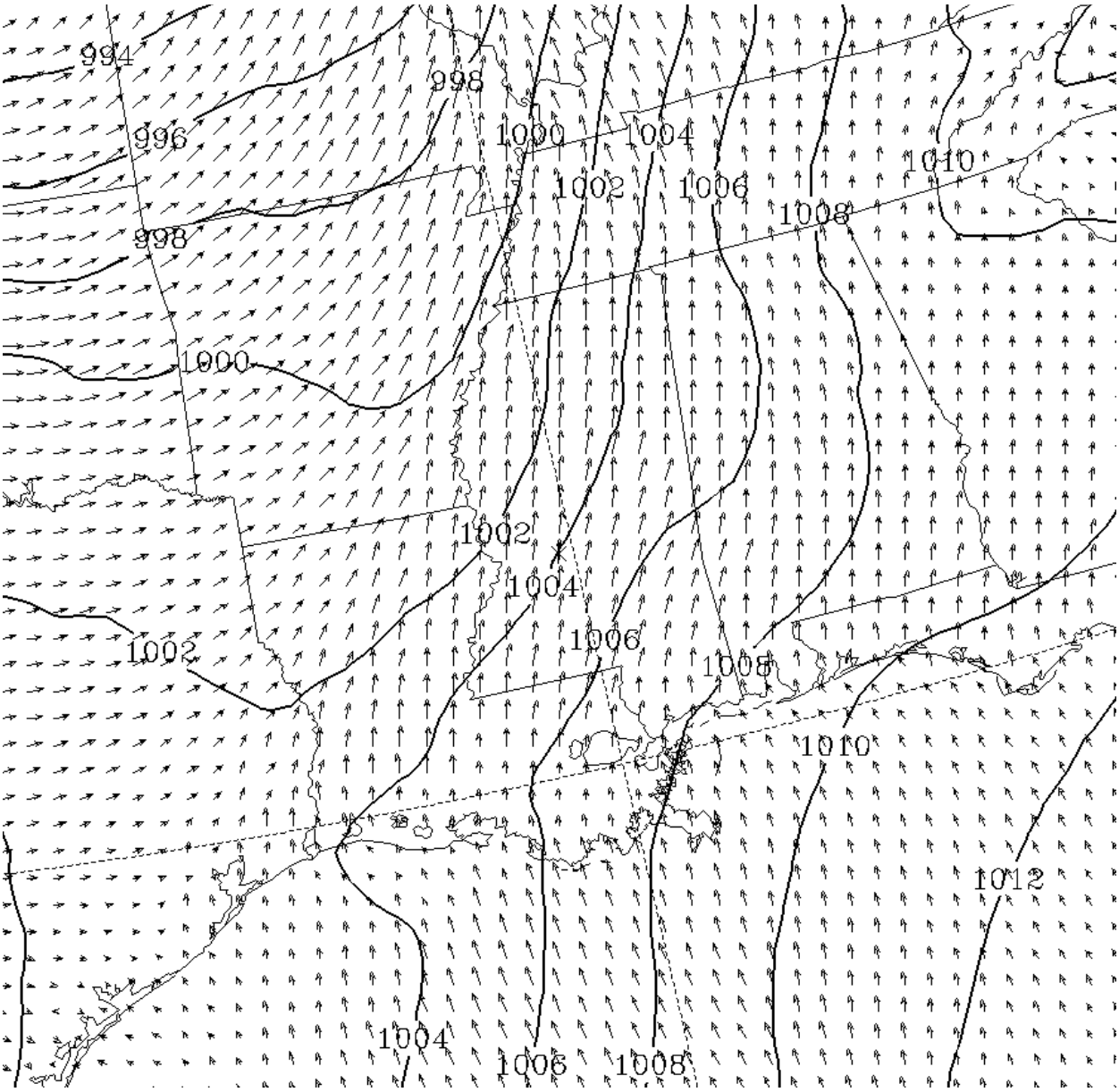

Figure 4.6. 2100 UTC 28 April 2014 plot showing mean seas level pressure (solid black contours) and wind vectors (black arrows). Notice the pronounced cross isobar flow across central Mississippi, indicating a likely region of enhanced storm relative helicity. Image courtesy of the Air Resources Laboratory.